Reliability and Failure Analyses of Thermally Cycled Ball Grid Array Assemblies

Reza Ghaffarian
Jet Propulsion Laboratory
California Institute of Technology
Pasadena, California
818-354-2059
Reza. Ghaffarian@JPL.NASA.Gov

Namsoo P. Kim
Boeing Information, Space & Defense Systems

ABSTRACT

Reliability of Ball Grid Arrays was assessed as part of a consortium effort led by the Jet Propulsion Laboratory. Nearly 200 test vehicles, each with four packages, were assembled and tested using an experiment design. The most critical variables incorporated in for the experiment were package types, ceramic and plastic; board materials, FR-4 and polyimide; surface finishes, OSP, HASL, and Ni/Au; solder volumes, low, standard, and high; and environmental conditions.

Two significantly different thermal cycle profiles were used at two facilities. The cycle A conditions ranged from -30 to 100°C and had increase/decrease heating rates of 2°C and dwells of about 20 minutes at the high temperature to assure near complete creeping. The duration of each cycle was 82 minutes. The cycle B conditions ranged from -55 to 125°C. Cycle B could be also considered a thermal shock since it used a three regions chamber: hot, ambient, and cold. Heating and cooling rates were nonlinear and varied between 10 to 15 °C/min. with dwells at extreme temperatures of about 20 minutes. The total cycle lasted approximately 68 minutes. BGA test vehicles were monitored continuously to detect electrical failure and their failure mechanism were characterized.

Thermal cycling test results to 3,000 cycles for ceramic packages with 625 I/Os and depopulated full array plastic packages with 313 I/Os were presented in a previous paper[1]. This paper will present the most current thermal cycling test results (>6,000 cycles) for plastic OMPAC and SuperBGA packages with 352 I/Os and 560 I/Os. Failure mechanisms detected by electrical continuity interruptions as well as optical and scanning electron microscopy results will also be compared for ceramic and plastic package assemblies.

WHY BGA

BGA is an important technology for utilizing higher pin counts, without the attendant handling and processing problems of the peripheral leaded packages. They are also robust in processing because of their higher pitch (0.050 inch typical), better lead rigidity, and self-alignment characteristics during reflow processing.

BGAs' solder joints cannot be inspected and reworked using conventional methods and are not well characterized for multiple double sided assembly processing methods. In high reliability SMT assembly applications, e.g. space and defense, the ability to inspect the solder joints visually has been standard and has been a key factor in providing confidence in solder joint reliability.

To address many common quality and reliability issues of BGAs, JPL organized a consortium with sixteen members in early 1995 [1]. Diverse membership including military, commercial, academia, and infrastructure sectors which permitted a concurrent engineering approach to resolving many challenging technical issues.

BGA TEST VEHICLE CONFIGURATION

The two test vehicle assembly types were plastic (PBGAs) and ceramic (CBGAs) packages. Both FR-4 and polyimide PWBs with six layers, 0.062 inch thick, were used.

Plastic packages covered the range from OMPAC (Overmolded Pad Array Carrier) to SuperBGAs (SBGAs). These were:

- Two peripheral SBGAs, 352 and 560 I/O
- Peripheral OMPAC 352 I/O, PBGA 352 and 256 I/O
- Depopulated full array PBGA 313 I/Os
- 256 QFP (Quad Flat Pack), 0.4 mm Pitch

In SBGA, the IC die is directly attached to an oversize copper plate providing better heat dissipation efficiency than standard PBGAs. The solder balls for plastic packages were eutectic (63Sn/37Pb).

Ceramic packages with 625 I/Os and 361 I/Os were also included in our evaluation. Ceramic solder balls (90Pb/10Sn) with 0.035 inch diameters had a high melting temperature. These balls were attached to the ceramic substrate with eutectic solder (63Sn/37Pb). At reflow, package side eutectic solder and the PWB side eutectic paste are reflowed to provide the electro-mechanical interconnects.

Plastic packages had dummy and daisy chains with the daisy chains on the PWB designed to be able to monitor critical solder joint regions. Most packages had four daisy chain patterns, 560 I/O package had five, and the QFP had one.

Package Dimensional Characteristics

Package dimensional characteristics are among the key variables that affect solder joint reliability. Dimensional characteristics of all packages were measured using a 3D laser scanning system for solder ball diameter, package warpage, and coplanarity [2].

Test Vehicle Assembling

Full assembly was implemented after process optimization from the trial test. The following procedures were followed:

- PWBs were baked at 125°C for four hours prior to screen printing.
- Two types of solder pastes were used, an RMA and a water soluble one.
- Pastes were screen printed and the heights were measured by laser profilometer. Three levels of paste were included in the evaluation: Standard, high, and low. Stencils were stepped to 50% to accommodate assembling ceramic, plastic, and fine pitch QFP packages in the Type 2 test vehicle.
- A 10 zone convection oven was used for reflowing.
- The first assembled Test Vehicle (TV) using an RMA reflow process was visually inspected and X-rayed to check solder joint quality.
- All assemblies were X-rayed

Two test vehicles were assembled:

- Type 1, ceramic and plastic BGA packages with nearly 300 I/Os.
- Type 2, ceramic and plastic BGA packages with nearly 600 I/Os. Also utilized were a 256 leaded ceramic and a 256 plastic BGA package for evaluating and directly comparing manufacturing robustness and reliability.
- Assemblies with water soluble flux were cleaned using an Electrovert H500. Those with RMAs were cleaned used Isopropyl Alcohol (IPA) and a 5% saponifier.
- All fine pitch QFPs had to be reworked for bridges.

THERMAL CYCLING

Two significantly different thermal cycle profiles were used at two facilities, conditions A and B. BGA test vehicles were continuously monitored through a LabView system at both facilities.

Failure Criteria

The criteria for an open solder joint specified in IPC-SM-785, Sect. 6.0, were used as guidelines to interpret electrical interruptions. Generally once the first interruption was observed, there were many additional interruptions within 10% of the cycle life. In several instances, a few non-consecutive early interruptions were not followed by additional interruptions until significantly later stages of cycling. This was found more with plastic packages.

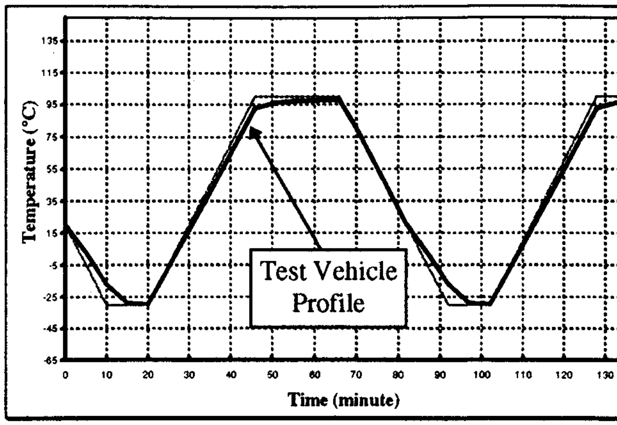

Figure 1 Thermal Profile for Condition A Thermal Cycling (-30°C to 100°C)

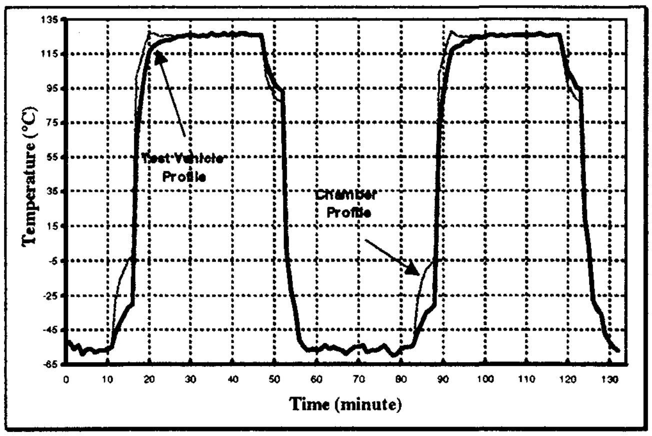

Figure 2 Thermal Profile for Condition B Thermal Cycle (-55°C to 125°C)

In Figure 3, the total number of electrical interruptions (daisy chain opens) are plotted vs number of cycles for cycle B condition. For ceramic BGAs, the rate of interruptions (slope) was approximately constant. This was not the case for the plastic BGAs. For a PBGA with 313 I/Os, the first interruption was at 913 cycles with no additional interruptions until about 3,000 cycles. Further erratic interruptions were observed between 3,000 and 3,700 cycles, followed with linear interruptions having approximately the same slope as the CBGAs. Another PBGA showed the first interruption at 3130 cycles and become open at about 3,300 cycles.

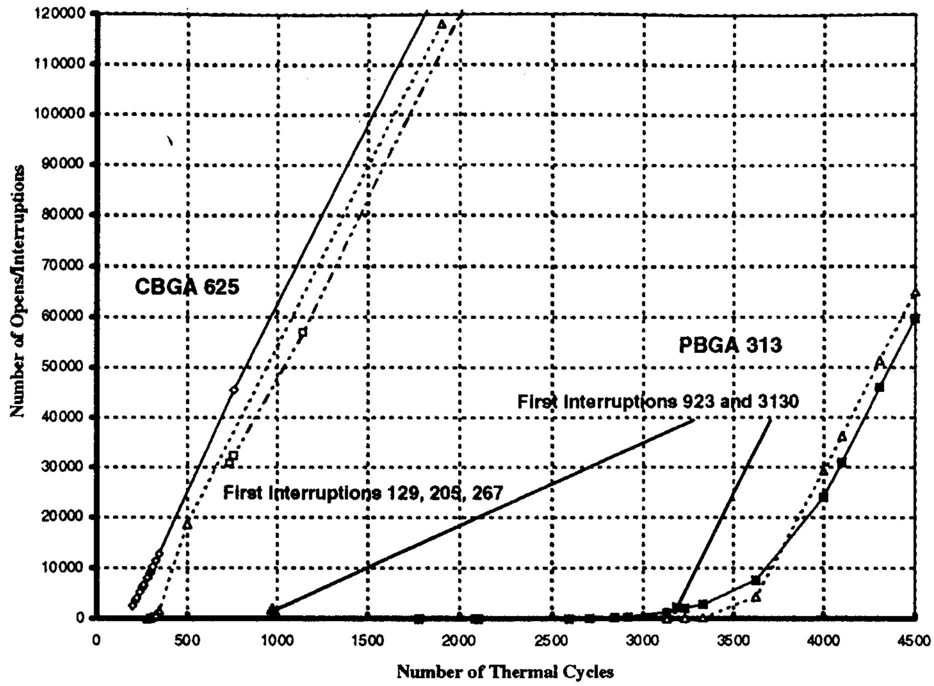

Figure 3 Number of Electrical Interruptions Detected with Thermal Cycles (-55°C to 125°C, B) for Ceramic and Plastic BGAs

Damage Monitoring

For conventional SMT solder joints, the pass/fail criteria for high reliability applications relies on visual inspection at 10x to 50x magnifications. For the BGAs on the test vehicles, only edge balls, those not blocked by other components, were visually inspected. A series of single assemblies which were cut from the test vehicles were also used for both visual and SEM inspection to better define visual criteria for acceptance of solder joints as well as to monitor damage progress under different cycling environments.

Failure Mechanism for Ceramic Assemblies

Figure 4 shows representative SEM and cross-sectional micrographs for a CBGA 625 package after 348 cycles of A conditions. Cross-section photos are for the perimeter balls, two corners and a center ball. SEM photos for package and board sides of a corner (maximum Distance to Neutral Point (DNP)) and the edge center ball are also included. Figure 5 compares the corner solder joint photo of Figure 4 and a typical failure photo for the B cycling conditions for a CBGA 361 package after 350 cycles. Note that the failures for the A conditions were from the PWB and for the B conditions were from the package sites. These were the typical failure mechanisms for the two conditions.

Failure mechanism differences could be explained by global or local stress conditions. Modeling indicates that the high stress regions shifted from the board to the package themselves when stress conditions changed from the global to local. The A cycling, with slow heat/cooling ramping, allowed the system to reach a uniform temperature, and damages could indicate a global stress condition. The B cycle damage, with rapid heat/cooling, could indicate a local stress condition.

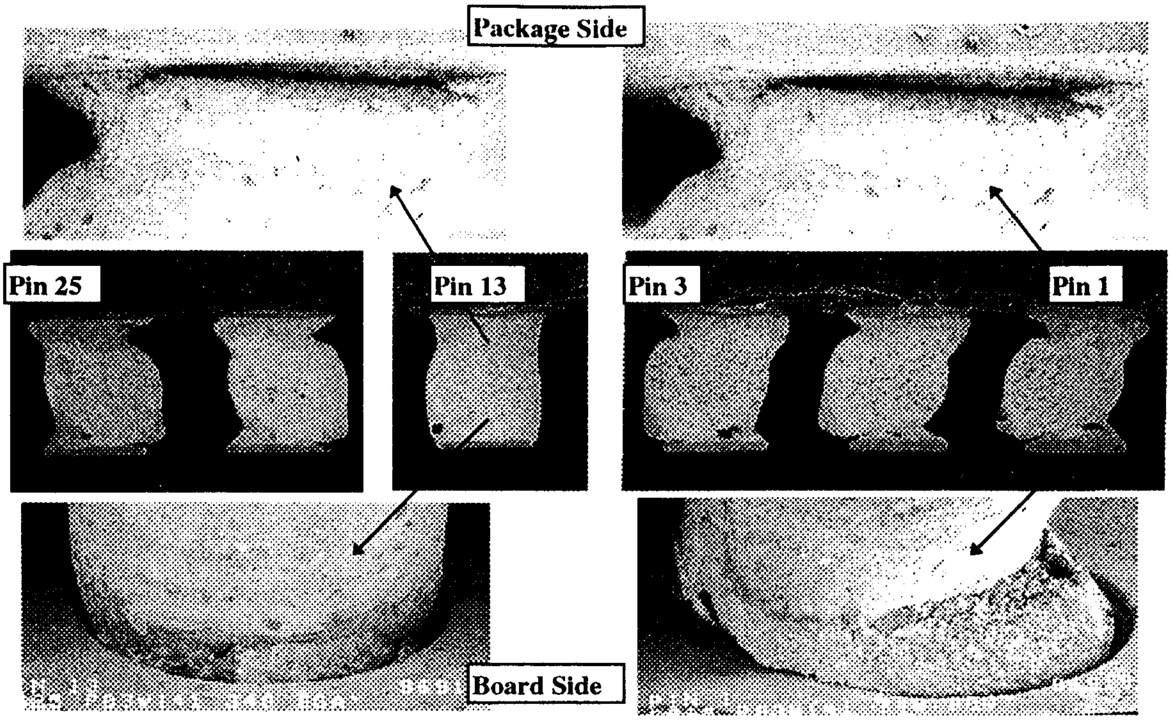

Figure 4 SEM and Cross-section photos for CBGA 625 after 348 cycles (-30°C to 100°C)

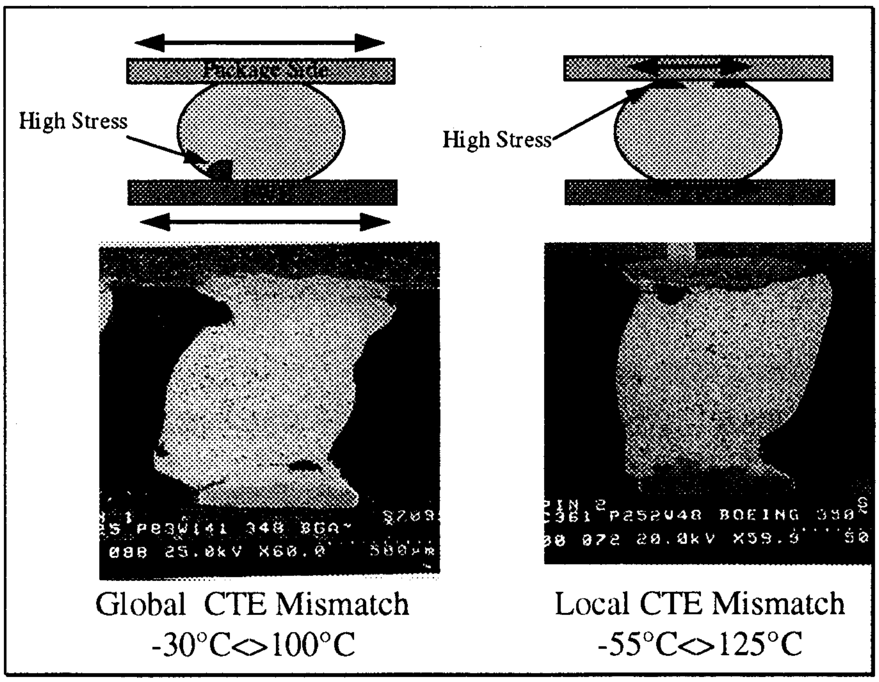

Figure 5 Cross-sections of Failure Sites for CBGA 625 after 350 cycles under A (-30°C to 100°C) and B Conditions

Failure Mechanisms for Plastic Assemblies

Among the plastic packages, the PBGA 313 with depopulated full array balls was first to fail under both B and A thermal cycling conditions. Figure 6 shows various cross-sections of this package's balls from corner to the center at 4,682 A cycles. These photos are for the balls under the die where most damages occur due to local CTE mismatch. Photos with and without voids were also included for comparison. Voids appear to have concentrated at the package interface under the die. Cracking propagation occurred at package or board interfaces for sections with or without voids.

The sections with voids were opens indicated by seepage of mounting materials into voids. Except for the interface connecting cracks, there appeared to be no crack propagation among the voids. The solder joints for this package were also visually inspected to identify indicators of defects. There were none apparent. Even when these were inspected at 100x by SEM, no gross damage was observed, as evidenced from the top left SEM photo of Figure 6.

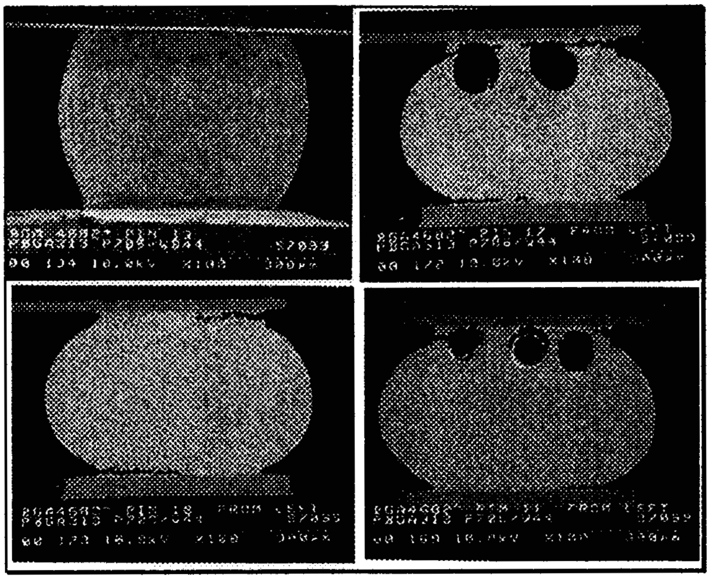

Figure 6 SEM and Cross-sections of PBGA 313 after

4,682 cycles under A (-30°C to 100°C) Conditions

Package attachment become very weak after 4,500 B cycles and could be easily detached from the board. Packages were detached and balls were inked and their images were mapped. The ball map distributions for several detached PBGA 313 I/O packages are shown in Figure 7. All joint failures were not from the board interface and there appeared to be a trend in their distribution.

For this depopulated full array package, most balls were separated from the package interface as evidenced from the low number of dark spots which represents the balls on the package. This is even more noticeable for the balls under the die. More joint failure at the package under the die portion could have occurred from the extreme local CTE mismatch at these joints. Similarly, mapping for other plastic packages was performed and trends are being studied. For ceramic packages, mapping was not possible since most of the packages were already separated from the board at 4,500 cycles. Failures were mostly at the package interface since detached packages generally had no balls on them. In addition, several test vehicle boards had a large number of balls remaining at the ceramic package locations.

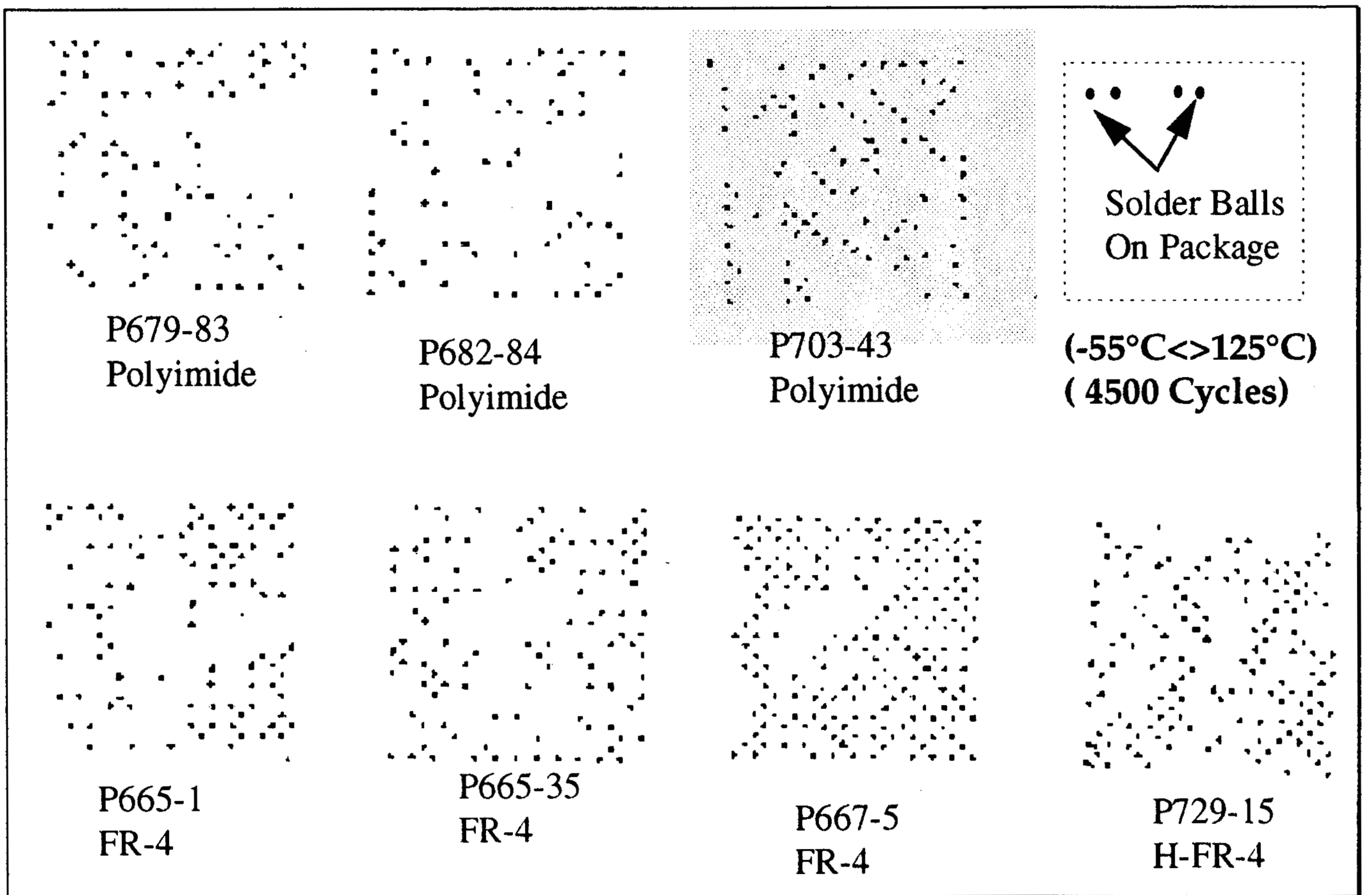

Figure 7 Maps of Solder Balls on PBGA 313 Packages after Detachment from Test Vehicle Assemblies after 4,500 B Cycles

Figure 8 shows cycles to first failure for four daisy chains of PBGA 313. The four daisy chains were for balls under the die, the edge die row, outer/inner rows, and the outer rows. As expected, the majority of the first cycles to failure were from the inner row, those under the die. Those lasted longest were from the outer rows. There were overlaps however in distribution and distinctions between sites of failure cannot be clearly defined. Similar plots were also generated for other packages.

For SBGA 352, package daisy chains were divided equally into four regions each covering a corner of the package. For this package, cycles to first failures were random from any of the four daisy chains. For the PBGA 256 and SBGA 560, both with peripheral array configuration, it appeared that cycles to first failures were not from the inner to outer rows.

THERMAL CYCLING RESULTS

Figure 9 shows cycles to first failure for all plastic packages: PBGA 313 and 256, OMPAC 352, SBGA 352 and 560. The results are for assemblies on FR-4 and Polyimide PWBs. Preliminary results for two assemblies showed generally higher cycles to failure for polyimide under the B conditions [1]. The most recent PBGA 313 assemblies that failed under the cycle A conditions are also included in the plots for comparison.

These plots were generated by ranking cycles to failures from low to high and then approximating the failure distribution percentiles using a median plotting position, $F_i = (i-0.3)/(n+0.4)$. No attempts were made to generate Weibull parameters since the sample sizes for B conditions was small and all assemblies under A conditions have not yet failed.

Several trends were identified. The PBGA 313, with a depopulated full array with solder balls under the die, were the first plastic packages to show signs of failure at both A and B cycling conditions. The scatter for both was narrow indicating large *m* Weibull parameter.

The next package assembly failure was SBGA 560. This package and the PBGA 256 with failure data at the extreme cycles showed very large scatter, indicating low *m* value. Scatter in PBGAs, in general, could be attributed to slow failure progress. Scatter in failure data for SBGA 560 could be due to the immaturity of the package at the time of use. These packages were taken from those assembled in the early stage of production. The reasons for a large scatter for the PBGA 256 cycles to failure data are not known at this time.

Cycles to failure data that are still being generated at JPL could shed some light on these and other plastic package failure behavior. Both OMPAC and SBGA 352 failed at later cycles than SBGA 560 was between a low tail for PBGA 313 and a high tail for PBGA 256. The 352 I/O package showed low scatter in cycles to failure data.

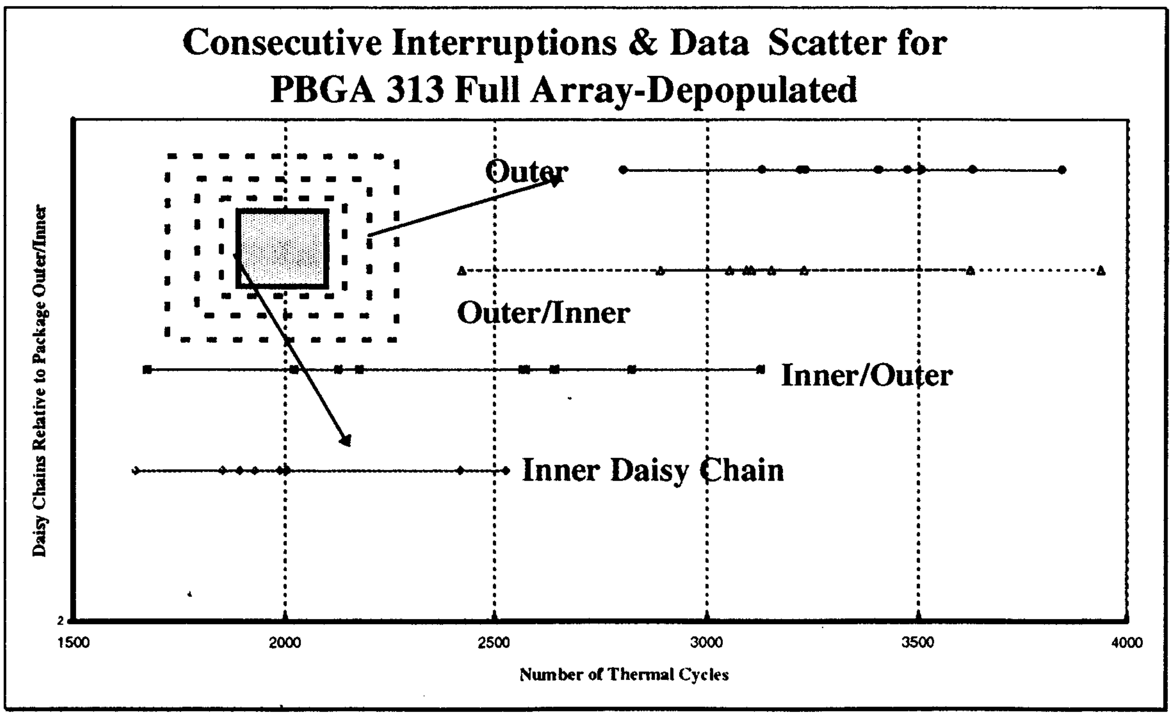

Figure 8 Cycles to First Failure for Inner to Outer Daisy Chains of PBGA 313

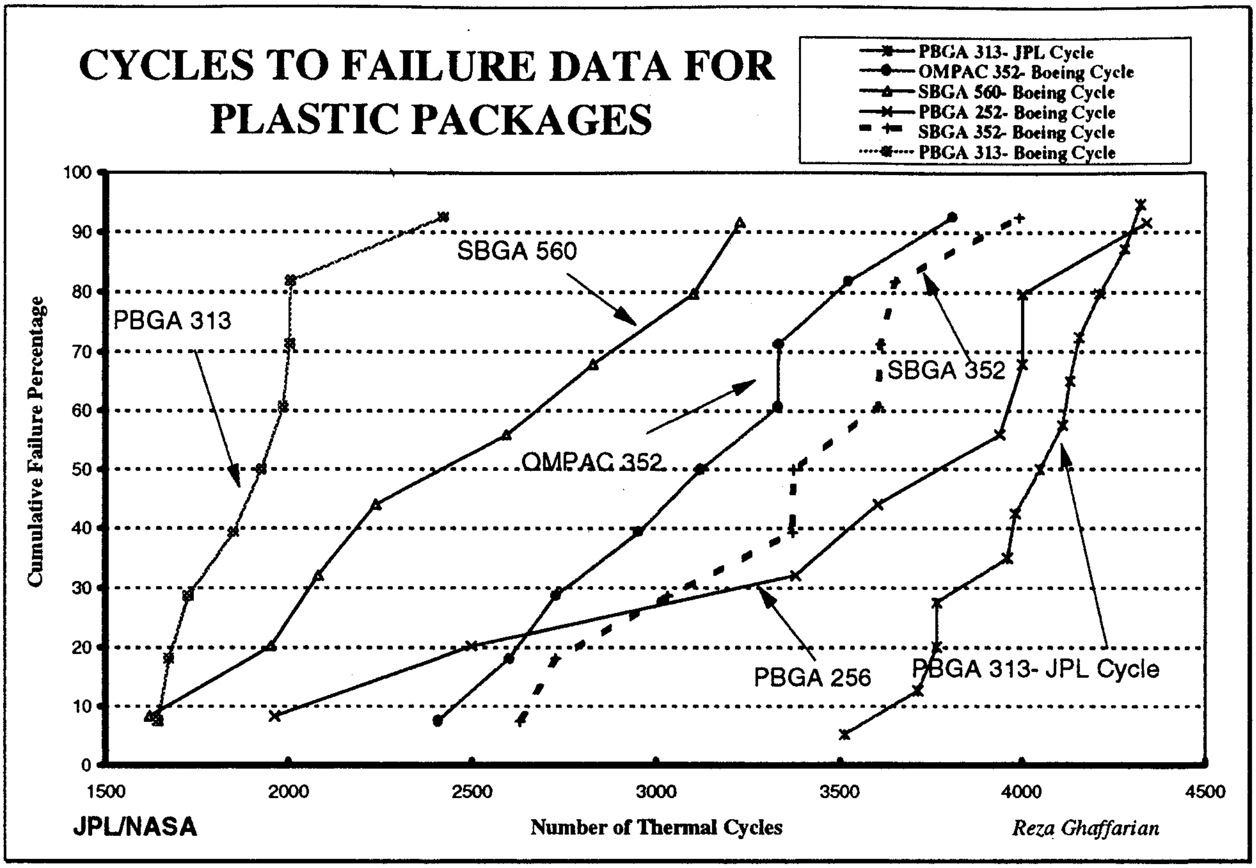

Figure 9 Cumulative Cycling to Failure for PBGA Assemblies (Cycle B) and PBGA 313 (Cycle A)

CONCLUSIONS

Failure Mechanisms

- Ceramic and plastic BGAs showed different failure mechanisms as evidenced from the total number of electrical interruptions with cycles. CBGAs showed linear correlations whereas PBGAs did not. For CBGAs, the first electrical interruption (open) was followed by consecutive additional interruptions. This was not the case for PBGAs, where the first interruption was not followed by additional interruptions until a much higher number of cycles.
- Joint failure mechanisms for assemblies exposed to the two cycling ranges A and B were different. Ceramic assemblies cycled in the range of -30°C to 100°C showed cracking initially at both interconnections and was separated from the board through the eutectic solder joints. The board joints showed signs of pin hole formation prior to crack initiations. This failure mechanism is similar to those reported in the literature for 0°C to 100°C thermal cycles.
- For plastic packages, crack propagations occurred at either the package or board interfaces for sections with or without voids. Generally, voids were concentrated near the package interfaces. There appeared to be no crack propagations among the voids, except for the voids interconnected at the interface.
- For PBGAs with 313 I/O depopulated full arrays, most of the initial failures were from the balls under the die, followed by failures at other regions. In some cases the failure distributions for the inner to outer regions were overlapped.
- For plastic assemblies, failures occurred either at the package or PWB interfaces for those examined after 4,500 B cycles. Failure sites were apparent visually on peripheral arrays and were evidenced from the missing balls on detached packages.

Assembly Reliability

- Plastic assemblies with I/Os from 254 to 560 on FR-4 and Polyimide PWBs, showed an order of magnitude larger number of cycles to failure than ceramic assemblies with I/Os from 361 to 625. They were in thousands of cycles for plastics whereas in hundreds for ceramics, in cycling temperature ranges of -55 to 125 °C and -30 to 100 °C.
- For ceramic assemblies, we were able to visually detect changes in the eutectic joints which could be used as early warning indicators for failures. This was not the case for the plastic assemblies. Indicators for CBGAs were due to differences in the metallurgy of ball and

solder and also because the first signs of damages occur in the corner joints with the highest DNP. The joints showed signs of grain growth, pin hole formation, creeping, microcracking and cracking prior to failure.

- Ceramic packages with 625 I/Os were first to show signs of failure among the ceramic (CBGA 361) and plastic packages (SBGA 560, SBGA 352, OMPAC 352, and PBGA 256) when cycled to different temperature ranges at the three facilities.
- The PBGAs with 313 I/O depopulated full arrays, were first among the PBGAs to fail (SBGA 560, SBGA 352, OMPAC 352, and PBGA 256) with both cycling ranges (A and B conditions). It has been well established that this configuration, with solder balls under the die, is not optimum from a reliability point of view.
- For peripheral plastic packages, the size and number of I/Os appeared to be the key factors in cycles to failure for B conditions. As the size increased, cycles to failure decreased, i.e., the SBGA 560 was first to fail in this category and PBGA 256 was the last. These two assemblies also showed a large scatter in cycles to failure. The reasons for the large failure scatters especially for the PBGA 256, are not well understood.
- Except for PBGA 313, there have been no failure of other plastic packages cycled in the range of -30° to 100°C up to 6,000 cycles.

REFERENCES

1. Ghaffarian, R., N. Kim, "Ball Grid Reliability Assessment for Aerospace Applications," 30th International Symposium on Microelectronics, Philadelphia, Pennsylvania, October 1997, pp. 396-400

ACKNOWLEDGMENTS

The research described in this publication is being carried out by the Jet Propulsion Laboratory, California Institute of Technology, under a contract with the National Aeronautics and Space Administration.

We would like to acknowledge the in-kind contributions and cooperative efforts of BGA consortium team members and those who had been contributors to the progress of the program.

Special thanks to Sharon Walton at JPL and David Bowen and Kevin Griffith at Boeing for monitoring the environmental testing. Our appreciation also goes to P. Barela, K. Evans, *JPL*; M. Simeus, *HMSC*; I. Sterian, *Celestica*; M. Andrews, *ITRI*; S. Levine, *Altron*; P. Mescher, *AMKOR*; M. Cole, and A. Trivedi, *IBM*.